Loss of Raf-1 Kinase Inhibitory Protein Delays Early-Onset Severe Retinal Ciliopathy in *Cep290^{rd16}* Mouse

Balajikarthick Subramanian,[1] Manisha Anand,[1] Naheed W. Khan,[2] and Hemant Khanna[1]

[1]Department of Ophthalmology, University of Massachusetts Medical School, Worcester, Massachusetts, United States
[2]Department of Ophthalmology & Visual Sciences, Kellogg Eye Center, University of Michigan, Ann Arbor, Michigan, United States

Correspondence: Hemant Khanna, Department of Ophthalmology, University of Massachusetts Medical School, 368 Plantation Street, Albert Sherman Center AS6-2043, Worcester, MA 01605, USA; hemant.khanna@umassmed.edu.

Submitted: June 5, 2014
Accepted: August 1, 2014

Citation: Subramanian B, Anand M, Khan NW, Khanna H. Loss of Raf-1 kinase inhibitory protein delays early-onset severe retinal ciliopathy in *Cep290^{rd16}* mouse. *Invest Ophthalmol Vis Sci*. 2014;55:5788–5794. DOI:10.1167/iovs.14-14954

Purpose. Mutations in the cilia-centrosomal protein of centrosomal protein of 290 kDa (CEP290) result in severe ciliopathies, including autosomal recessive early onset childhood blindness disorder Leber congenital amaurosis (LCA). The *Cep290^{rd16}* (retinal degeneration 16) mouse model of CEP290-LCA exhibits accumulation of CEP290-interacting protein Raf-1 kinase inhibitory protein (RKIP) prior to onset of retinal degeneration (by postnatal day P14). We hypothesized that reducing RKIP levels in the *Cep290^{rd16}* mouse will delay or improve retinal phenotype.

Methods. We generated double mutant mice by combining the *Cep290^{rd16}* and *Rkip^{ko}* alleles (*Cep290^{rd16}:Rkip$^{+/ko}$* and *Cep290^{rd16}:Rkip$^{ko/ko}$*). Retinal function was assessed by ERG and retinal morphology and protein trafficking were assessed by histology, transmission electron microscopy (TEM), and immunofluorescence analysis. Cell death was examined by apoptosis.

Results. Prior to testing our hypothesis, we examined ERG and retinal morphology of *Rkip$^{ko/ko}$* mice and did not find any detectable differences compared with wild-type mice. The *Cep290^{rd16}:Rkip$^{+/ko}$* mice exhibited similar retinopathy as *Cep290^{rd16}*; however, *Cep290^{rd16}:Rkip$^{ko/ko}$* double knockout mice demonstrated a substantial improvement (>9-fold) in photoreceptor function and structure at P18 as of *Cep290^{rd16}* mice. We consistently detected transient preservation of photoreceptors at P18 and polarized trafficking of opsins to sensory cilia in the double mutant mice; however, retinal degeneration ensued by P30.

Conclusions. Our studies implicate CEP290-RKIP pathway in CEP290-retinal degeneration and suggest that targeting RKIP levels can delay photoreceptor degeneration, assisting in extending the time-window for treating such rapidly progressing blindness disorder.

Keywords: CEP290, RKIP, retina, photoreceptor degeneration, blindness

Cilia are microtubule-based membrane extensions that act as antenna to sense the extracellular environment. They are formed by docking of the mother centriole (basal body) at the apical plasma membrane followed by recruitment of multiprotein complexes, including small GTPases and microtubule motor proteins. Microtubules extend from the basal body into a short structure called the transition zone, which acts as a "gatekeeper" by forming Y-linkers that connect the microtubules to the plasma membrane. Cilia then extend further into the extracellular milieu in the form of axoneme.[1–6]

Photoreceptors are polarized sensory neurons that develop a sensory cilium in the form of photosensory outer segment (OS).[2,7–10] The OS consists of stacks of membranous discs that are periodically shed and renewed daily. This process involves enormous polarized protein trafficking from the inner segment (where protein synthesis takes place) to the OS via a narrow transition zone (or connecting cilium). The OS is a hub for opsin and other proteins involved in phototransduction cascade. Even subtle defects in the stringently regulated protein and membrane trafficking machinery result in photoreceptor degeneration and blindness.[11–15]

Centrosomal protein of 290 kDa (CEP290) is a cilia-centrosomal protein involved in regulating cilia formation and protein trafficking in photoreceptors and other cell types.[16–19] Mutations in CEP290 result in a range of defects, likely dependent upon the extent of loss of CEP290 function. Mutations in CEP290 are implicated in perturbing the gatekeeping function of the transition zone of cilia[18,20–22] and are frequently (20%–25%) associated with childhood blindness disorder, Leber congenital amaurosis type 10 (LCA10; MIM 611755).[23–26] Also, CEP290 mutations are relatively common in other syndromic ciliopathies with variable and systemic clinical manifestations, such as Joubert syndrome, Meckel-Gruber syndrome, and Bardet-Biedl syndrome.[5,6,27]

Animal models of CEP290 mutations offer crucial insights into its function and associated pathogenesis. A naturally occurring cat model of CEP290 mutation was reported earlier, which exhibits a relatively delayed onset retinal defect.[28] We previously reported the characterization of *rd16* (retinal degeneration 16) mouse carrying an in-frame deletion in *Cep290*.[20] This mouse exhibits early onset severe photoreceptor dysfunction and degeneration, starting as early as postnatal day P14. The mutant CEP290 protein is still expressed at detectable levels in the mutant mouse. In addition to retinal degeneration, the *Cep290^{rd16}* mouse exhibits other sensory deficits, such as anosmia and hearing abnormalities.[20,22] However, no other systemic ciliopathies, such as kidney or cerebellar defects, were observed.

In addition to providing valuable insights into the function of CEP290, the *Cep290^{rd16}* mouse is an excellent platform to

test therapeutic strategies. We had earlier reported that CEP290 interacts with Raf-1 Kinase Interacting Protein (RKIP) and that this interaction is perturbed in the *Cep290*^{rd16} mouse retina.[18] Moreover, there is aberrant accumulation of RKIP in photoreceptors prior to onset of retinal degeneration. These observations suggest that accumulation of RKIP is associated with the pathogenesis in the *rd16* mouse. Therefore, we hypothesized that modulating RKIP levels in the *Cep290*^{rd16} mouse can mitigate retinal degeneration. In this report, we assessed the effect of loss of RKIP on the progression of photoreceptor dysfunction and degeneration in the *Cep290*^{rd16} mouse by generating and characterizing double mutant mice. Our studies provide a novel tool to design supplemental therapies for successfully rescuing rapidly progressing retinal degeneration due to CEP290 mutations.

Materials and Methods

Animals

All animal experiments were performed with prior approval and in compliance with the Institutional Animal Care and Use Committee regulations. Mice were maintained and bred with unrestricted access to water and food in the same light conditions (10–15 lux), and in a 12-hour light and 12-hour dark cycle. Both *Cep290*^{rd16} [20] and *Rkip*$^{ko/ko}$ (a gift of Kam Yeung, University of Toledo, Toledo, OH, USA)[29] mice on C57BL6/J background were used to generate double-mutant *Cep290*^{rd16}:*Rkip*$^{ko/ko}$, and single heterozygote mutant of *Rkip*, *Cep290*^{rd16}:*Rkip*$^{+/ko}$. The mutations were confirmed by both genotyping PCR and retina specific immunoblot using previously described procedures.[20,29] The list of primers used for the characterization of mouse models with their primer annealing temperature and expected PCR product size can be made available upon request.

Immunoblotting

Mice ($n = 5$) eyes were enucleated and the retinas were lysed and sonicated in radio immunoprecipitation assay buffer (Cell Signaling Technology, Beverly, MA, USA) with protease inhibitors (Roche, Inc., Nutley, NJ, USA). The protein extracts were collected by centrifugation at 13,000*g* for 15 minutes at 4°C and analyzed by SDS-PAGE and immunoblotting, as described.[14]

Antibodies

Commercial antibodies included anti-RKIP (Millipore Corp., Billerica, MA, USA), anti-rhodopsin (Millipore Corp.), anti-β-tubulin (Sigma-Aldrich Corp., St. Louis, MO, USA), and anti-CEP290 (Bethyl Labs, Montgomery, TX, USA). Anti-M opsin was a gift of Cheryl M. Craft.[42] Secondary antibodies included AlexaFluor 488 and AlexaFluor 546 (Molecular Probes, Eugene, OR, USA).

ERG, Histology, and Immunofluorescence

Analyses with ERG were performed using a commercial diagnostic technique (Espion Diagnosys LLC, Cambridge, UK) as described previously.[14] For histology and immunofluorescence, mouse eyes were enucleated, fixed in 4% paraformaldehyde (PFA) overnight at 4°C, ethanol-dehydrated in serial gradients, and embedded as paraffin blocks. Sections of 7-μM thickness were cut along the vertical meridian of each eyeball and stained with H&E.

For immunofluorescence staining, mouse eyes were fixed in 4% PFA, cryoprotected in 30% sucrose overnight and frozen in optimal cutting temperature (OCT) compound (Tissue-Tek; Sakura Finetek, Torrance, CA, USA); 20-μM sections were used for staining as described previously.[14] All images were captured using a commercial imaging system (Leica DMI6000B; Leica Microsystems, Wetzlar, Germany).

Morphometric Analysis

The morphometric analysis of outer nuclear layer (ONL) thickness in *Cep290*^{rd16} and *Cep290*^{rd16}:*Rkip*$^{ko/ko}$ was performed as described.[14] Sections of H&E along the optic nerve head (ONH) plane from five different mice were used for measurements.

Transmission Electron Microscopy (TEM)

For ultrastructural analysis using TEM, mouse eyes were treated and as described.[14] Briefly, eyes were enucleated and fixed in 2.5% glutaraldehyde in 0.1 M sodium cacodylate buffer (pH 7.2) overnight at 4°C. The eyecups were then washed three times in 0.1 M sodium cacodylate buffer, postfixed in 1% osmium tetroxide/0.1 M cacodylate buffer, ethanol dehydrated, and then finally embedded in epoxy resin. Ultrathin sections (70 nm) were cut along the vertical meridian of eyeball with ONH using an ultramicrotome (Leica Reichart-Jung; Leica Microsystems) and stained with 2% uranyl acetate and 4% lead citrate. The resulting retina sections were then visualized with a TEM (Philips CM-10; Philips, Eindhoven, The Netherlands), coupled with a charge-coupled device digital camera (Gatan Erlangshen 785; Gatan, Inc., Warrendale, PA, USA).

TUNEL Staining

Staining with TUNEL was performed using a commercial kit (ApopTag Plus fluorescein In Situ Apoptosis Detection Kit; Chemicon International, Temecula, CA, USA). Briefly, paraffin sections were deparaffinized, pretreated with proteinase K, stained using fluorescein conjugated digoxigenin/antidigoxigenin system, and counterstained using DAPI. The mounted sections were then imaged and quantified for apoptotic cells.

Statistical Analyses

All statistical analyses were carried out using graphing software (GraphPad Prism Version 6.0; GraphPad, Inc., La Jolla, CA, USA). Data were analyzed using one-way ANOVA and when statistical significance was seen by ANOVA, the Tukey's comparison of means was used to find significant group differences. Statistical significance was set at minimal value of $P < 0.05$. All graphical representations of data were also generated in graphing software (GraphPad, Inc.).

Results

Retinal Function in *Rkip*$^{ko/ko}$ Mice

We first evaluated the expression of RKIP protein in the *Rkip*$^{ko/ko}$ [29] mouse retina. While we detected the expected ~25 kDa anti-RKIP immunoreactive band in wild-type retinal extracts, the *Rkip*$^{ko/ko}$ retinal extract did not exhibit an immunoreactive band (Fig. 1A). To test the effect of ablation of *Rkip* on retinal morphology and function, we assessed retinal histology and photoreceptor function of the *Rkip*^{ko} mice. Hematoxylin and eosin (H&E) staining of retinal sections or transmission electron microscopy (TEM) did not reveal any differences in the development of the retinal layers in the mutant mice compared with age-matched wild-type mice (Figs. 1B, 1C). Consistently, ERG analysis of rod and cone photoreceptor function also did not reveal any detectable differences between *Rkip*^{ko} and wild-type mice (data not shown). Overall, these results show that ablation of *Rkip* has no detectable effect on retinal development and function.

Investigative Ophthalmology & Visual Science

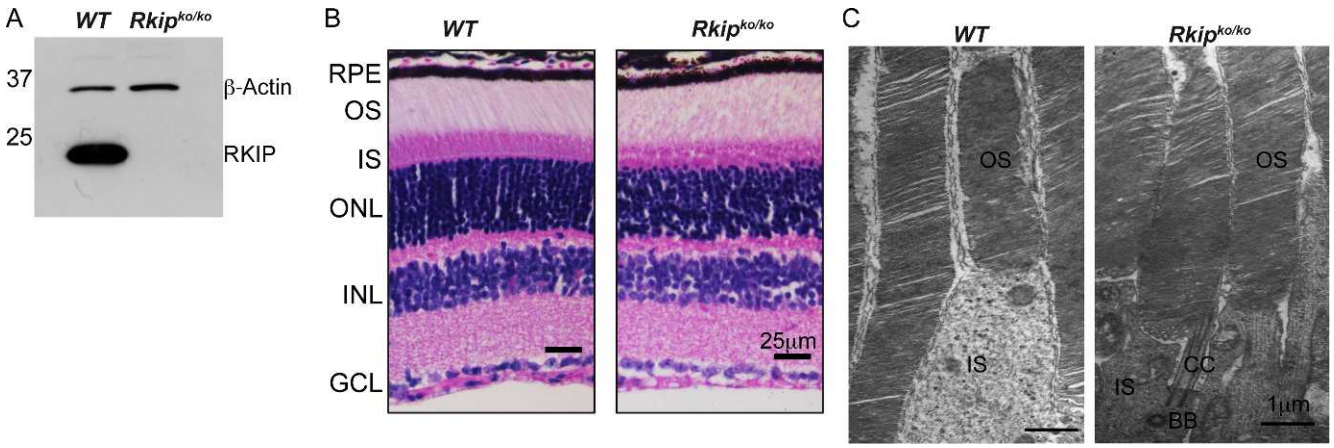

Figure 1. Characterization of *Rkip*$^{ko/ko}$ mice. **A**. Immunoblot analysis of retinal extracts (30 μg) was performed using anti-RKIP or anti-β-actin antibody (loading control). Molecular mass markers are shown on the left in kDa. (**B**, **C**). Histological (**B**) and TEM (**C**) analysis of WT and *Rkip*$^{ko/ko}$ retina was performed as described in the "Materials and Methods" section. BB, basal body; CC, connecting cilium; GCL, ganglion cell layer; INL, inner nuclear layer. *Scale bars*: 25 μm (**B**), 1 μm (**C**).

Characterization of *Cep290*^{rd16}:*Rkip*$^{ko/ko}$ Double-Mutant Mice at P18

We then generated double-mutant mice by breeding *Cep290*^{rd16} mice with *Rkip*$^{ko/ko}$ mice. Both mouse strains are on C57BL6/J background. Immunoblot analysis of the mutant mouse retinas validated the expression of the deleted variant (shorter protein band) of CEP290 in the *Cep290*^{rd16} as well as *Cep290*^{rd16}:*Rkip*$^{ko/ko}$ double-mutant mice (Fig. 2A). As predicted, RKIP protein expression was not detected in the *Rkip*$^{ko/ko}$ and double-mutant mice (Fig. 2A). Notably, no change in RKIP protein levels was detected in *Cep290*^{rd16}:*Rkip*$^{+/ko}$ mice compared with *Cep290*^{rd16} mice; and as predicted,[18] the RKIP protein levels are significantly increased in these mice compared with the wild-type (WT) mice (Fig. 2A; lower panel).

Further analysis of the double-mutant mice showed that loss of RKIP in the *Cep290*^{rd16} mice results in relative preservation

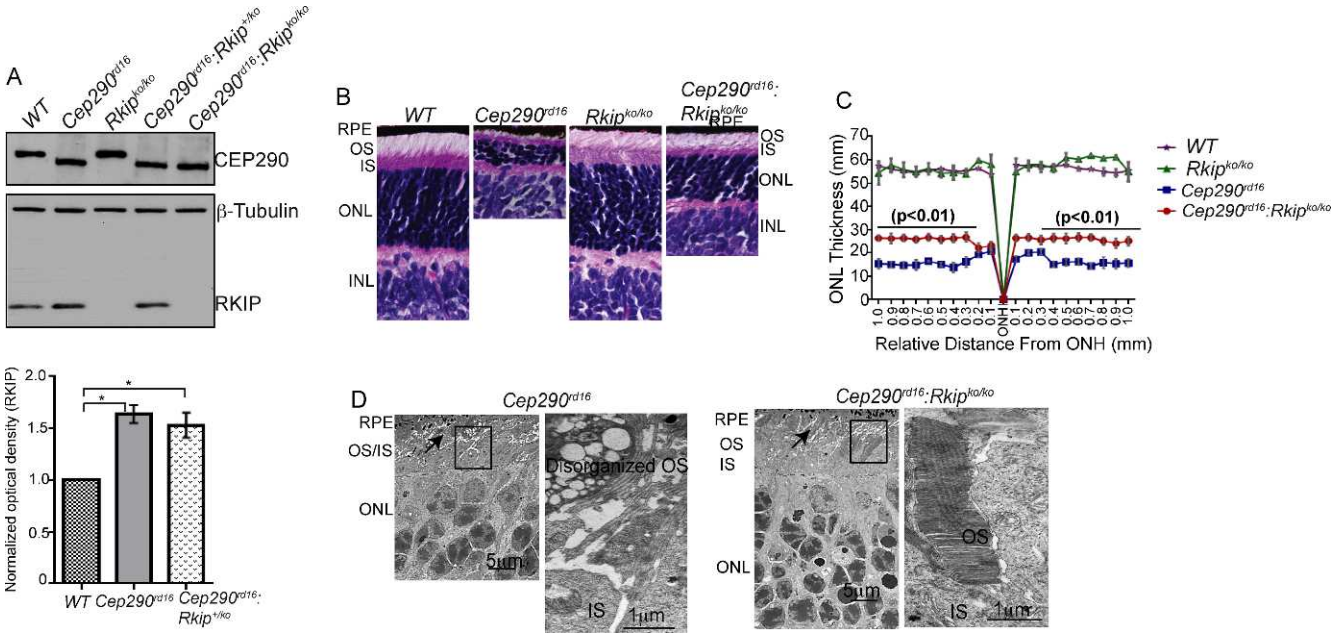

Figure 2. Characterization of double-knockout mice. (**A**) Immunoblot analysis of retinal extracts (30 μg) of mice of indicated genotypes was performed using antibodies against CEP290, RKIP and β-tubulin (loading control); RKIP immunoreactive band is not detected in the *Rkip*$^{ko/ko}$ lanes. Also, predicted shorter deleted variant of CEP290 is detected in *Cep290*^{rd16} retinal extract. *Lower panel* shows quantitative analysis of the band intensity of RKIP in the *Cep290*^{rd16} and *Cep290*^{rd16}:*Rkip*$^{+/ko}$ mouse retina relative to WT. (**B**) Histological analysis of WT and mutant retinas of indicated genotypes was performed to assess retinal morphology. Thinning of the ONL was observed in the *Cep290*^{rd16} retina, whereas improved thickness of the ONL is detected in the *Cep290*^{rd16}:*Rkip*$^{ko/ko}$ retina. (**C**) Morphometric analysis of retinas, also showed an overall statistically significant ($P < 0.01$) improvement in the thickness of the ONL. Retinas from five different mice of each genotype were analyzed in this experiment. (**D**) TEM analysis of *Cep290*^{rd16} (*left panel*) and *Cep290*^{rd16}:*Rkip*$^{ko/ko}$ (*right panel*) mice was performed to assess detailed photoreceptor morphology. *Arrow* in *upper panel* points to indistinguishable OS and IS while *arrow* in *lower panel* depicts organized OS and IS. *Inset* shows disorganized OS in *Cep290*^{rd16} photoreceptors and correctly developed and stacked OS discs in *Cep290*^{rd16}:*Rkip*$^{ko/ko}$ retina. *Scale bars*: 5 and 1 μm (*inset*).

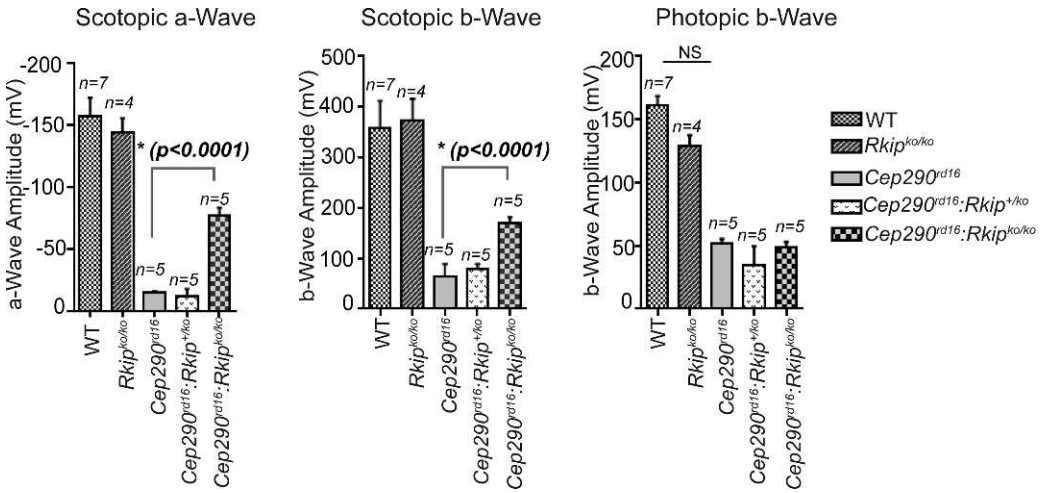

Figure 3. Electroretinography of mutant mice at P18. Scotopic (dark-adapted) and photopic (light-adapted) ERG was performed in mice of indicated genotypes. Light-adapted ERGs were recorded using a background white light illumination of 34 cd/m^2 for 8 minutes. A single step stimulus of 10 cd/m^2 was used and an average from 20 trials was presented as photopic response. Statistically significant improvement in scotopic A- and B-wave amplitudes was detected in *Cep290*^{rd16}:*Rkip*$^{ko/ko}$ mice compared with *Cep290*^{rd16} mice. NS, statistically nonsignificant. *$P < 0.0001$.

of retinal morphology by P18. Histological analysis showed increase in the thickness of photoreceptor outer nuclear layer (ONL; Fig. 2B). Morphometric analysis further validated these findings. It revealed an approximately 2-fold increase in the thickness of the ONL in the double-mutant mice compared with *Cep290*^{rd16} mice (Fig. 2C; $P < 0.01$). The WT and *Rkip*$^{ko/ko}$ mice showed comparable thickness of the ONL (Fig. 2C). We then performed ultrastructural analysis of photoreceptors of the different mutant mice. As shown in Figure 2D, *Cep290*^{rd16} retina exhibits disorganized OS and indistinguishable OS and inner segment (IS) layers, whereas *Cep290*^{rd16}:*Rkip*$^{ko/ko}$ double-mutant retina shows a well-formed OS structure with stacked discs and distinguishable IS.

Functional Analysis of Double-Mutant Mice

We next tested the effect of ablation of *Rkip* in *Cep290*^{rd16} mice on the function of photoreceptors. Measurement of ERG responses revealed improved rod photoreceptor function in dark-adapted conditions at P18 in the double-mutant mice compared with *Cep290*^{rd16}. As shown in Figure 3, scotopic (dark-adapted) A-wave amplitude revealed >9-fold increased response ($P < 0.0001$) while B-wave increased by ~2-fold ($P < 0.0001$). No improvement was detected in *Cep290*^{rd16}:*Rkip*$^{+/ko}$ indicating that complete loss of RKIP is important for the observed improvement in *Cep290*^{rd16} mouse retina. Interestingly, measurement of photopic B-wave responses at P18 did not reveal an improvement in the double-mutant mice.

Protein Trafficking in Double-Mutant Mice

We then assessed the effect of loss of RKIP in *Cep290*^{rd16} on the trafficking of opsins to OS. While almost complete mislocalization of rhodopsin and cone opsin was detected in the *Cep290*^{rd16} retina at P18, the double-mutant mice exhibited improved trafficking of the opsins to the OS (Fig. 4). As predicted, WT and *Rkip*$^{ko/ko}$ mice did not show a mislocalization of opsins.

Retinal Phenotype of Double-Mutant Mice at P30

We next tested whether the preservation of retinal structure and function is stable over longer time periods in the double-mutant mice. To this end, we performed histological and ERG analyses of the *Cep290*^{rd16} and *Cep290*^{rd16}:*Rkip*$^{ko/ko}$ mice at age 1 month (P30). Surprisingly, we detected deterioration in retinal morphology and function (Fig. 5). Intriguingly, although *Cep290*^{rd16} showed a considerable decline in photopic B-wave amplitude by P30, ~20% increase in the B-wave amplitude was detected in *Cep290*^{rd16}:*Rkip*$^{ko/ko}$ at the same age (Fig. 5A). The increase in the B-wave amplitude was transient as shown by decrease in the signal at P60 in the double knockout mice,

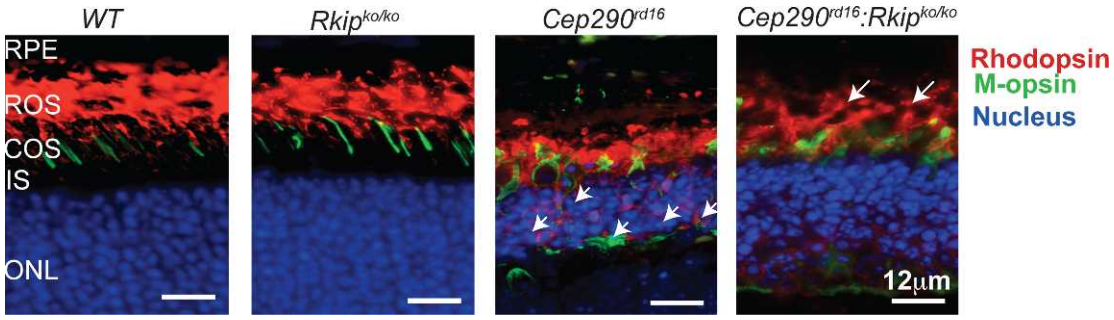

Figure 4. Trafficking of OS proteins at P18. Cryosections from WT and mutant mice were stained for rhodopsin (*red*; rods) and M-opsin (*green*; cones). Nuclei were stained with Hoechst (*blue*). *Arrows* indicate bulk of rhodopsin signal in the OS of *Cep290*^{rd16}:*Rkip*$^{ko/ko}$ mice, whereas *small arrows* indicate considerable rhodopsin mislocalization in the ONL of *Cep290*^{rd16} mice. *Rkip*$^{ko/ko}$ retina did not exhibit a difference in opsin trafficking as compared to WT. *Scale bars*: 12 μm.

Investigative Ophthalmology & Visual Science

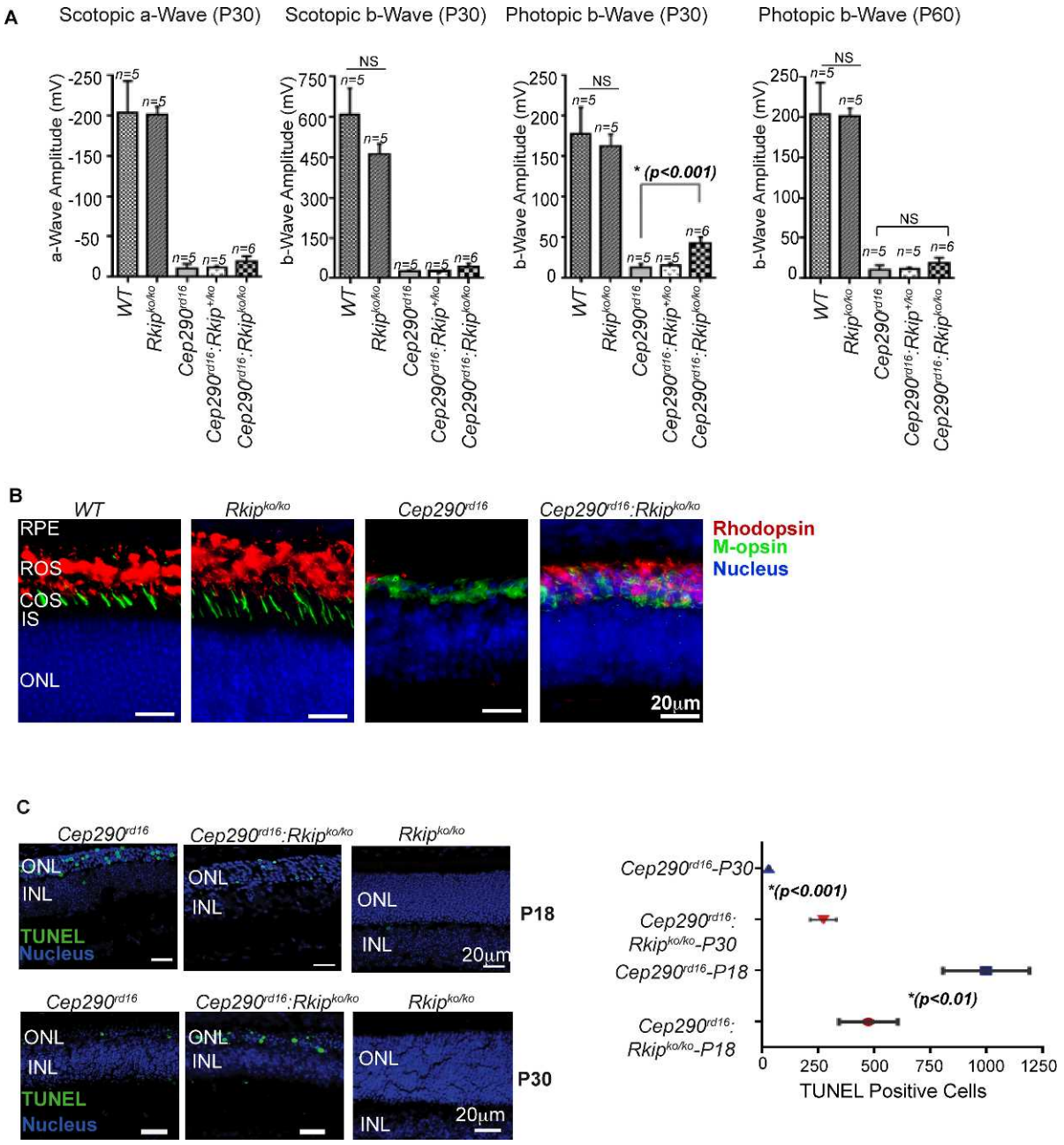

Figure 5. Characterization of mutant mice at P30 and P60. Analysis of ERG (**A**) and immunofluorescence analysis (**B**) were performed as described in the Materials and Methods section. Rhodopsin (*red*) and M-opsin (*green*) antibodies were used for staining at P30 (B). Nuclei were stained with Hoechst (*blue*). (**C**) Cell death at P18 and P30 was assessed by TUNEL staining (*green*) of retinas of indicated genotypes. Graphical representation from three different experiments of number of TUNEL-positive (*green*) cells in the ONL is depicted on the right. Nuclei are stained with Hoechst (blue). *Scale bars*: 20 μm. Number of mice in (A) is indicated as *n*. *$P < 0.001$.

which was comparable with the B-wave amplitude of *Cep290*^{rd16} at the same age. Rhodopsin-positive photoreceptors with relatively improved trafficking were still detectable in the double-mutant mice compared with *Cep290*^{rd16} at P30, indicating overall slower degeneration in the *Cep290*^{rd16}:*Rkip*$^{ko/ko}$ mice (Fig. 5B).

Photoreceptor Cell Death in Double-Mutant Mice

We then asked whether improved photoreceptor structure and function is associated with decrease in cell death. To this end, we performed TUNEL staining of retinas of different genotypes. As shown in Figure 5C, we found significantly reduced TUNEL-positive nuclei in the outer nuclear layer in the *Cep290*^{rd16}:*Rkip*$^{ko/ko}$ mice compared with *Cep290*^{rd16} ($P < 0.01$) at P18. As control, very few TUNEL-positive cells were present in *Rkip*$^{ko/ko}$ mouse retina. Staining with TUNEL at P30 (Fig. 5C) revealed that cell death in the *Cep290*^{rd16} mouse retina was almost completed and very low levels of TUNEL-positive nuclei were observed. Nonetheless, cell death continued at P30 in the *Cep290*^{rd16}:*Rkip*$^{ko/ko}$ retina and we observed significantly high number of TUNEL-positive nuclei in the ONL compared with *Cep290*^{rd16} ($P < 0.001$) at P30, but reduced TUNEL-positive nuclei compared with P18. Overall, these results indicate a

transient rescue in phenotype and a continued but delayed degeneration of photoreceptors in the double knockout mice.

Discussion

Leber congenital amaurosis (LCA; MIM 204000) is one of the most severe forms of congenital blindness disorders.[25,26] Over 13 genes have now been identified to be associated with autosomal recessive LCA cases. Gene therapeutic strategies for LCA have shown promise both in animal models and in patients who develop moderate visual impairment at infancy progressing into total blindness by mid to late adulthood.[30–33] Mutations in CEP290 result in relatively early onset severe retinal degeneration and dysfunction in mice and humans. The fast progression of the disease makes it difficult to pinpoint the stage at which therapeutic intermediates can be implemented. Our studies reported here show that retinal degeneration in the *Cep290^{rd16}* mouse can be delayed by downregulating the expression of RKIP, potentially making it amenable to other therapeutic paradigms. Such intermediates can be used in combination with other strategies, such as antisense oligonucleotide therapy for CEP290 mutations,[34] to improve the outcome of the treatment.

Intracellular levels of other CEP290-interacting proteins such as BBS6 and BBS4 have been shown to positively or negatively affect the phenotype of the *rd16* mouse.[22,35] However, it should be noted that these proteins are involved in human ciliopathies and that modulating their levels as a therapeutic paradigm can have negative effects. Loss of RKIP, on the other hand, does not seem to perturb development or survival of photoreceptors. Therefore, RKIP and other such proteins are potentially suitable candidates for targeted therapy to delay photoreceptor death. As RKIP is involved in regulating MAP Kinase signaling,[36] further studies on the role of these pathways in modulating photoreceptor development and survival should also provide candidate pathway intermediates that can be used in combination with other therapeutic strategies.

Although we observed increased thickness of the ONL at P18, the increase in scotopic A-wave and B-wave responses at P18 did not improve to WT levels. This suggests that although there is increased survival of photoreceptors in the *Cep290^{rd16}:Rkip$^{ko/ko}$* mice, they may not be completely normal and may still possess trafficking defects as well as stress due to severity of the disease in the absence of functional CEP290. Such results further inform about the complexities associated with CEP290-associated retinal degeneration. Our observation of delayed but significant preservation of cone function as detected by photopic B-wave at P30 is probably due to an indirect effect of sustained retinal health because of increase in the surviving rod photoreceptors. In fact, we also detect rod photoreceptors at P30 although their function is considerably reduced in the *Cep290^{rd16}:Rkip$^{ko/ko}$* mice. However, we cannot rule out a specific effect of loss of RKIP in cones in the *Cep290^{rd16}* mouse that results in a delayed improvement in cone function. Previous studies have shown that CEP290 mutations can have differential effects on cones, indicating a distinct role of CEP290, and potentially its interacting proteins, in these cell types.[37] Further studies are needed to assess these scenarios in a cell-type specific manner.

The results presented here point to a role of CEP290 in modulating RKIP levels for normal photoreceptor development and survival. It has been shown that RKIP is degraded via the ubiquitin-proteasome system (UPS).[38] Given the involvement of cilia and basal body proteins in regulating the UPS,[39,40] it is conceivable that CEP290 targets RKIP to the UPS. Elegant recent studies have shown that proteasomal dysfunction due to overload of proteins being targeted to degradation can be a common underlying mechanism in multiple models of retinal degeneration.[41] Therefore, it is possible that reduction in RKIP levels assists in reducing the load on the proteasome and results in a slight improvement in photoreceptor survival. Additional investigations are needed to clearly dissect the role of CEP290 in maintaining the levels of RKIP in the retina.

A transient delay in retinal degeneration in the absence of RKIP in the *Cep290^{rd16}* mice indicates involvement of additional pathways that culminate in photoreceptor dysfunction and degeneration. Further studies hold promise of identification of other RKIP-like CEP290-interacting proteins or additional pathways involving CEP290 that can be modulated to retain the ability to improve photoreceptor health in disease.

Acknowledgments

The authors thank Gregory Pazour and George Witman (UMASS Medical School), Carlos A. Murga-Zamalloa (University of Michigan), and Rivka A. Rachel (National Eye Institute) for helpful discussions; and Garrett Grahek (University of Michigan) for assistance with ERG; UMASS Cell Biology Confocal Core and Electron Microscopy Core (Award # S10RR027897).

Supported by grants from Foundation Fighting Blindness (HK) and National Eye Institute (EY022372; HK). The authors alone are responsible for the content and writing of the paper.

Disclosure: **B. Subramanian**, None; **M. Anand**, None; **N.W. Khan**, None; **H. Khanna**, None

References

1. Doxsey S. Re-evaluating centrosome function. *Nat Rev Mol Cell Biol*. 2001;2:688–698.
2. Insinna C, Besharse JC. Intraflagellar transport and the sensory outer segment of vertebrate photoreceptors. *Dev Dyn*. 2008; 237:1982–1992.
3. Mazelova J, Astuto-Gribble L, Inoue H, et al. Ciliary targeting motif VxPx directs assembly of a trafficking module through Arf4. *EMBO J*. 2009;28:183–192.
4. Nachury MV, Seeley ES, Jin H. Trafficking to the ciliary membrane: how to get across the periciliary diffusion barrier? *Annu Rev Cell Dev Biol*. 2010;26:59–87.
5. Nigg EA, Raff JW. Centrioles, centrosomes, and cilia in health and disease. *Cell*. 2009;139:663–678.
6. Novarino G, Akizu N, Gleeson JG. Modeling human disease in humans: the ciliopathies. *Cell*. 2011;147:70–79.
7. Besharse JC, Baker SA, Luby-Phelps K, Pazour GJ. Photoreceptor intersegmental transport and retinal degeneration: a conserved pathway common to motile and sensory cilia. *Adv Exp Med Biol*. 2003;533:157–164.
8. Liu Q, Tan G, Levenkova N, et al. The proteome of the mouse photoreceptor sensory cilium complex. *Mol Cell Proteomics*. 2007;6:1299–1317.
9. Murga-Zamalloa C, Swaroop A, Khanna H. Multiprotein complexes of retinitis pigmentosa GTPase regulator (RPGR), a ciliary protein mutated in x-linked retinitis pigmentosa (XLRP). *Adv Exp Med Biol*. 2010;664:105–114.
10. Yildiz O, Khanna H. Ciliary signaling cascades in photoreceptors. *Vision Res*. 2012;75:112–116.
11. Besharse JC, Hollyfield JG. Renewal of normal and degenerating photoreceptor outer segments in the Ozark cave salamander. *J Exp Zool*. 1976;198:287–302.
12. Besharse JC, Hollyfield JG, Rayborn ME. Photoreceptor outer segments: accelerated membrane renewal in rods after exposure to light. *Science*. 1977;196:536–538.

13. Deretic D, Schmerl S, Hargrave PA, Arendt A, McDowell JH. Regulation of sorting and post-Golgi trafficking of rhodopsin by its C-terminal sequence QVS(A)PA. *Proc Natl Acad Sci U S A*. 1998;95:10620–10625.
14. Li L, Khan N, Hurd T, et al. Ablation of the X-linked retinitis pigmentosa 2 (Rp2) gene in mice results in opsin mislocalization and photoreceptor degeneration. *Invest Ophthalmol Vis Sci*. 2013;54:4503–4511.
15. Young RW. Passage of newly formed protein through the connecting cilium of retina rods in the frog. *J Ultrastruct Res*. 1968;23:462–473.
16. Anand M, Khanna H. Ciliary transition zone (TZ) proteins RPGR and CEP290: role in photoreceptor cilia and degenerative diseases. *Exp Opin Ther Tar*. 2012;16:541–551.
17. Kim J, Krishnaswami SR, Gleeson JG. CEP290 interacts with the centriolar satellite component PCM-1 and is required for Rab8 localization to the primary cilium. *Hum Mol Genet*. 2008;17:3796–3805.
18. Murga-Zamalloa CA, Ghosh AK, Patil SB, et al. Accumulation of the Raf-1 kinase inhibitory protein (Rkip) is associated with Cep290-mediated photoreceptor degeneration in ciliopathies. *J Biol Chem*. 2011;286:28276–28286.
19. Tsang WY, Bossard C, Khanna H, et al. CP110 suppresses primary cilia formation through its interaction with CEP290, a protein deficient in human ciliary disease. *Dev Cell*. 2008;15:187–197.
20. Chang B, Khanna H, Hawes N, et al. In-frame deletion in a novel centrosomal/ciliary protein CEP290/NPHP6 perturbs its interaction with RPGR and results in early-onset retinal degeneration in the rd16 mouse. *Hum Mol Genet*. 2006;15:1847–1857.
21. Craige B, Tsao CC, Diener DR, et al. CEP290 tethers flagellar transition zone microtubules to the membrane and regulates flagellar protein content. *J Cell Biol*. 2010;190:927–940.
22. Rachel RA, May-Simera HL, Veleri S, et al. Combining Cep290 and Mkks ciliopathy alleles in mice rescues sensory defects and restores ciliogenesis. *J Clin Invest*. 2012;122:1233–1245.
23. den Hollander AI, Koenekoop RK, Yzer S, et al. Mutations in the CEP290 (NPHP6) gene are a frequent cause of Leber congenital amaurosis. *Am J Hum Genet*. 2006;79:556–561.
24. den Hollander AI, Roepman R, Koenekoop RK, Cremers FP. Leber congenital amaurosis: genes, proteins and disease mechanisms. *Prog Retin Eye Res*. 2008;27:391–419.
25. Estrada-Cuzcano A, Roepman R, Cremers FP, den Hollander AI, Mans DA. Non-syndromic retinal ciliopathies: translating gene discovery into therapy. *Hum Mol Genet*. 2012;21:R111–R124.
26. Koenekoop RK. An overview of Leber congenital amaurosis: a model to understand human retinal development. *Surv Ophthalmol*. 2004;49:379–398.
27. Badano JL, Mitsuma N, Beales PL, Katsanis N. The ciliopathies: an emerging class of human genetic disorders. *Annu Rev Genomics Hum Genet*. 2006;7:125–148.
28. Menotti-Raymond M, David VA, Schaffer AA, et al. Mutation in CEP290 discovered for cat model of human retinal degeneration. *J Hered*. 2007;98:211–220.
29. Theroux S, Pereira M, Casten KS, et al. Raf kinase inhibitory protein knockout mice: expression in the brain and olfaction deficit. *Brain Res Bull*. 2007;71:559–567.
30. Acland GM, Aguirre GD, Ray J, et al. Gene therapy restores vision in a canine model of childhood blindness. *Nat Genet*. 2001;28:92–95.
31. Cideciyan AV, Hauswirth WW, Aleman TS, et al. Human RPE65 gene therapy for Leber congenital amaurosis: persistence of early visual improvements and safety at 1 year. *Hum Gene Ther*. 2009;20:999–1004.
32. Maguire AM, High KA, Auricchio A, et al. Age-dependent effects of RPE65 gene therapy for Leber's congenital amaurosis: a phase 1 dose-escalation trial. *Lancet*. 2009;374:1597–1605.
33. Pawlyk BS, Bulgakov OV, Liu X, et al. Replacement gene therapy with a human RPGRIP1 sequence slows photoreceptor degeneration in a murine model of Leber congenital amaurosis. *Hum Gene Ther*. 2010;21:993–1004.
34. Collin RW, den Hollander AI, van der Velde-Visser SD, Bennicelli J, Bennett J, Cremers FP. Antisense oligonucleotide (AON)-based therapy for Leber Congenital Amaurosis caused by a frequent mutation in CEP290. *Mol Ther Nucleic Acids*. 2012;1:e14.
35. Zhang Y, Seo S, Bhattarai S, et al. BBS mutations modify phenotypic expression of CEP290-related ciliopathies. *Hum Mol Genet*. 2014;23:40–51.
36. Al-Mulla F, Bitar MS, Taqi Z, Yeung KC. RKIP: much more than Raf kinase inhibitory protein. *J Cell Physiol*. 2013;228:1688–1702.
37. Cideciyan AV, Aleman TS, Jacobson SG, et al. Centrosomal-ciliary gene CEP290/NPHP6 mutations result in blindness with unexpected sparing of photoreceptors and visual brain: implications for therapy of Leber congenital amaurosis. *Hum Mutat*. 2007;28:1074–1083.
38. Qu Y, Dang S, Hou P. Gene methylation in gastric cancer. *Clin Chim Acta*. 2013;424:53–65.
39. Gerdes JM, Liu Y, Zaghloul NA, et al. Disruption of the basal body compromises proteasomal function and perturbs intracellular Wnt response. *Nat Genet*. 2007;39:1350–1360.
40. Liu YP, Tsai IC, Morleo M, et al. Ciliopathy proteins regulate paracrine signaling by modulating proteasomal degradation of mediators. *J Clin Invest*. 2014;124:2059–2070.
41. Lobanova ES, Finkelstein S, Skiba NP, Arshavsky VY. Proteasome overload is a common stress factor in multiple forms of inherited retinal degeneration. *Proc Natl Acad Sci U S A*. 2013;110:9986–9991.
42. Zhu X, Brown B, Li A, Mears AJ, Swaroop A, Craft CM. GRK1-dependent phosphorylation of S and M opsins and their binding to cone arrestin during cone phototransduction in the mouse retina. *J Neurosci*. 2003;23:6152–6160.

Investigative Ophthalmology & Visual Science